



## Comparative Histomorphological and Adaptational Study of the Respiratory System in Male Albino rat and Pigeon

Shahad Fadhil Ahmed Mohammed<sup>1\*</sup>, Shurooq Hameed Majeed Alnassiri<sup>2</sup>

<sup>1,2</sup> Department of Biology, College of Education for Women, University of Tikrit-Iraq .  
EMAIL: shaha.Ahmead841@st.tu.edu.iq<sup>1</sup>, shurooq\_bio@tu.edu.iq<sup>2</sup>

### Abstract

**Background:** One of the best examples among this incredible variety is found in vertebrate respiratory systems such as those that have evolved to match some very high-level demands for metabolism specific to environmental niche and these styles reside at either advantageous ends on a continuum with non-homogenous conductance features driving tidal (mammals) vs. non-tidal, alveolar (birds) functionality expressed accordingly.

**Aim:** The present study was aimed at a comparative histomorphological examination of male albino rat (*Rattus norvegicus*) and domestic pigeon respiratory tract (*Columba livia*), so as to visualize some specific structural differences which can bring functional adaptations.

**Materials and Methods:** Tissues from adult male samples (n=10 per group) were obtained [topographically distinct respiratory segments of the larynx, trachea, syrinx, lungs]. Serial sections of  $\mu$  m thick were prepared and stained with Hematoxylin and Eosin (H&E) for microscopic eye morphometric analysis.

**Results:** These histomorphological differences were apparent in every organ that was studied. Mammals possess a larynx which consists of vocal cords, an epiglottis covered with stratified squamous and respiratory epithelia; in contrast avian cranial larynxes lack both Vocal cords and Epiglottis all at the same time. Supporting the rat trachea were C-shaped hyaline cartilage rings completed only posteriorly by smooth muscle. By contrast, their trachea was made of complete O-shaped rings knitted together by partial ossification and hyaline cartilage to resist the rigors of flying. Notably, the pigeon possessed a paired voice box (syrinx) at tracheal bifurcation enabled with specialized vibrating membranes and flexible syringeal cartilages. The most obvious differences related to pulmonary architecture: the rat lung showed a typical mammalian bronchioalveolar paradigm with terminal alveoli whereas the pigeon lung featured an expansible parenchyma dominated by interconnected parabronchi and highly vascularised air capillaries linking many hundreds of cavities into complex cross-current gas exchange apparatuses.

**Conclusions:** The results reveal that, despite functioning as efficient gas exchangers for both species, their respective microscopic structure points to evolutionarily divergent strategies. The pigeon shows very rigid, tubular and continuous-flow airways more consistent with a specialized avian respiratory system when compared to the tidal compliant mammalian rat.

**Keywords:** Histomorphology; Respiratory System; *Rattus norvegicus*; *Columba livia*; Syrinx; Evolution.

### Introduction

The respiratory system is one of the most complex physiological systems in vertebrates and serves as an important interface for oxygen uptake and carbon dioxide removal while maintaining homeostasis under dynamic conditions. One of the few fields that captures functional coincident evolutionary and adaptive specialization among species of animals (Moussavi, 2022) is comparative respiratory morphology which interdigitate with intraspecific variation within organ structure.

Vertebrate evolutionary lineage respiratory structures have taken on extremely diverse forms in response to environmental constraints, metabolic demands and locomotor needs. Most notably, these adaptations have resulted in a remarkable diversity of respiratory architecture (Dekan et al., 2020), especially in endothermic vertebrates that require augmented gas exchange to meet the bioenergetic demands associated with higher levels of metabolic activity (Phyu et al.).

The clearer relationship between structure and function is reinforced at higher metabolic activity rates. Indeed in respiratory muscles, similar adaptations to optimize ventilation and gas transport at wide-ranging physiologic conditions are eyewitnessed (Dominelli & Sheel 2024) because efficient pulmonary functioning is actually key during enhanced oxygen demands that occur with movement exercise.

White rat (*Rattus norvegicus*) is the most popular mammal animal models for anatomical and biomedical research, it has been widely used in many studies. With a bronchial tree and large lobes of the carina, rats possess an excellent mammalian structure for tidal ventilation (Rekabdar et al., 2024).

The mammalian lung is histologically characterized by a highly ramified structure of bronchioles, alveolar ducts and alveoli lined with specialized pneumocytes. This increases the area of respiratory exchange surface and minimizes diffusion distance from air to blood (and vice versa; Mulka et al., 2026).

Heterogeneity in the network of alveolar walls is a significant regulator of both airflow repartition and pulmonary tissue mechanics, as recently revealed through observations. Furthermore, such subtle heterogeneity is fundamental for respiratory function and highlights the significant role histological organisation plays in pulmonary efficiency (Tsuda & Henry 2023).

The morphological characteristics of air–blood barrier also play a large role in regulating oxygen diffusion and pulmonary fluid homeostasis. This barrier has different thickness and composition, therefore is regarded as an important regulator of pulmonary function and a major adaptive mechanism in mammalian lungs (Miserocchi 2023).

Birds, unlike mammals, have an intricate respiratory system that has been described as the most-efficient among all living vertebrates. Many of the other organ systems are affected as well (Maina, 1989), including birds which have a comparatively rigid pulmonary structure coupled with an elaborate air sac system that preserves unidirectional flow through alveolar lungs throughout inspiration and expiration allowing for maximal oxygen uptake under their specific high energetic needs associated with flight (Maina 2025).

These structures]] evolved along the birds evolutionary history from air sacs and neopulmo to more specifically specialized cass of respiratory system with basic functions fulfilling pulmonary ventilation role that are required for performance as one of the most efficient terrestrial animal respirators. These are differences in evolution that started making claims for birds as distinct amongst the vertebrate forms (Klein et al., 2025).

Avian - One of the most amazing feature of avian respiration system is its lungs allow for unidirectional flow through parabronchial lung. The configuration works to provide continuous flow of oxygenated air over the gas-exchange surfaces during both inspiratory and expiratory events; unlike bidirectional tidal breathing (which is characteristic in mammals); such that respiration can be maximally efficient (Schachner & Moore, 2025).

There is also a remarkable anatomical and histological difference across mammals and birds in the upper respiratory tract. In mammals, as in the case of true vocal folds (referred to simply as "vocal folds" for simplicity) within larynxes of white rat mesentery and gland tissue always providing live support duct systems involved with both airway protections phonation. On the other hand, unlike mammals birds have a separated and rather trivial cranial larynx but use an evolutionary adaptation of their tracheobronchial system (resize) – namely diffusion activation through syrinx for vocalisation which shows different ways in how evolution can drive respiratory function as well as sound production or reproduction(Ritchison 2023)..

## Materials and Methods

### 1.Ethical Statement and Experimental Design

The protocol of this comparative study was reviewed and approved by the education Institutional Animal Care and Use Committee According to the Animal Ethics Guideline of the College of Veterinary Medicine/Tikrit University, A total of twenty adult healthy male specimens-ten white albino rats (*Rattus norvegicus*) with ages 6-24 months and ten domestic pigeons (*Columba livia*) Ages 6-12 months-were utilized, All animals were housed under standard controlled laboratory conditions, maintained on a 12 -hour light/dark cycle at a temperature of  $23 \pm 25^{\circ}\text{C}$ , and provided with species-specific nutrition commercial pellets and water ad libitum

### 2. Animal Euthanasia and Tissue Harvesting

To minimize suffering and preserve optimal tissue architecture, all specimens were humanely euthanized using an overdose of anesthesia, All the experimental animals were anesthetized in the same way, Each animal in the groups was anesthetized by placing it in a tightly sealed plastic container containing a piece of cotton soaked in the anesthetic chloroform, and leaving it for a short period until the animal stopped moving (Padmanahban *et al.*, 1981), Following confirmation of clinical death, immediate ventral midline incisions were performed to expose the respiratory tract, For the rats, the cranial larynx, trachea, and both lung lobes were systematically excised, For the pigeons, the cranial larynx, the complete long trachea, the tracheobronchial syrinx (caudal voice box), and both deeply embedded, non-lobed lungs were gently dissected out without crushing the delicate parenchymal boundaries .

### 3. Tissue Fixation and Processing

Immediately upon surgical extraction, all isolated tissue specimens were washed with chilled normal saline (0.9% NaCl) to remove residual blood clots. Harvested organs were immersed in greater than 10 times their volume of 10% neutral buffered formalin (NBF) for atleast >48 hours RT to allow complete tissue cross-linking/fixation and stabilization. This involved a series of successive dehydration treatments in ascending concentration gradient 70%,80% chemical fixation step followed by the second dehydration treatment with absolute alcohols ( $\geq 90\%$ ,  $100\%$  each  $\geq 2$  h thereafter per station). Dehydrated specimens were completely

evacuated of ethyl alcohol using a series-modified technique in two solvents of pure xylene and subsequently infiltrated with molten histological grade paraffin wax (56–58 °C) under vacuum.

#### 4. Microtomy and Block Sectioning

The paraffin-infiltrated samples were carefully oriented and embedded into solid paraffin blocks to allow for precise cross-sectional and longitudinal structural viewing. A total of ten high-quality paraffin blocks were selected and designated per specific respiratory organ for each animal cohort to fulfill thorough regional sampling criteria. Microtomy was executed using a semi-automated rotary microtome; serial her type is LKB, sequential thin sections were cut uniformly at a thickness of 6 µm, The resulting floating ribbon sections were gently stretched and mounted onto clean, premium glass slides using a warm distilled on Fisher type water bath maintained at 35-40°C and Then the sections were loaded onto glass slides marked with a diamond pen with the name of the organ, and placed on a Reichert-type hot plate at a temperature of (40)°C until they dried, then left for 24 hours.

#### 5. Histological Staining Protocol

The mounted tissue sections were processed through standard progressive Harris's hematoxylin and alcoholic eosin (H&E) staining to evaluate generalized tissue morphology, structural layer differentiation, and cellular outlines, Briefly, The paraffin wax was completely removed from the sections using hot xylene (45)°C, whereby the slides with the sections attached were passed through two changes of xylene for (3 minutes each) until the wax was completely removed from the slides, and rehydrated via a descending ethanol gradient (100%, 90%, 70% 50%) down to distilled water, Slides were stained with Harris Hematoxylin for 5 minutes, rinsed in running tap water, Then It passed through distilled water for (3) minutes, Afterwards, I passed the sections through an alcoholic eosin stain solution for (2) minutes, Then I washed twice with ethyl alcohol at increasing concentrations of 70%, 80%, 90%, and up to 100% for (3) minutes each time. Finally, the stained slides were rapidly dehydrated in absolute ethanol, cleared via pure xylene changes, and permanently mounted with DPX hydrophobic mounting medium under clean glass coverslips .

#### 6. Microscopic Examination and Histomorphometric Analysis

All prepared histopathology specimens (representing the 10 reference slide replicates per anatomical segment) were systematically scanned and examined using an advanced Compound Optical/Light Microscope research-grade light microscope equipped with a high-definition digital camera, The Digital photomicrographs is captured at varying optical magnifications (40x, 100 x, and 400 x) and then Used a Microscopy Camera Eyepiece for PC 0.3M Pixel DCE-PW1 for tissue sections, connected to a Lenovo ThinkPad X1 Carbon laptop, to reveal tissue architectures, luminal epithelial linings, and protective cartilaginous configurations and else, Then the photos were printed using a color printer and glossy photo paper, and by means of an EPSON Styls TX210 color printer.

### Results

#### Histomorphological Findings of the Respiratory System in Male Albino rat (*Rattus norvegicus*)

##### Nasal Cavity

Histological examination of the nasal cavity in male albino rat revealed that the vestibular region was lined by keratinized stratified squamous epithelium resting on a well-developed lamina propria composed of dense collagenous connective tissue containing numerous blood vessels and scattered inflammatory cells (Figure 1). Within the dermal layer, epithelial papillae extending into underlying connective tissue and appearing with hair follicles and collagen fibers typical of nasal integument were also present (Figures 2,3).

Many mucous glands with basally located nuclei and pale secretory cytoplasm in deeper regions of the nasal cavity. Their high-density lobes were situated within a stroma of connective tissue containing collagen fibers, blood capillaries and dispersed leukocytes. Apart from this, serous glands were also seen in few portions of the nasal mucosa (figs 4 and 5). Also, submucosal connective tissue exhibited large venous plexuses and infrequent lymphoid aggregates (Figures 6,7)

##### Larynx and Trachea

Rat laryngeal wall was defined by clusters of cartilage throughout isolated with a perichondrium and joined to bundles of skeletal muscle strands and collagenous connective tissue (Figures 8,9,10). The cartilage matrix was rich in chondrocytes within regular lacunae, and the surrounding connective tissue showed scattered leukocytes and macrophages.

Histological sections of the trachea revealed a pseudostratified columnar respiratory epithelium overlaid on loose connective tissue comprising lamina propria, with inserted blood vessels and infiltrate macrophages/leukocytes. The submucosal showed smooth muscle and was continued with big cartilage hyaline rings surrounded by a fibrous perichondrium (Figures 11, mean12). The outer adventitial layer was composed of loose connective tissue with adipocytes, inflammatory cells, and collagen fibers (Figure 13) Well-defined hyaline cartilage rings filled up well-developed chondrocytes aggregated around whole circumference wall in

the trachea to form densely packed slices that blended into one another along Spindle axes for maintain supportive characteristics (figure 14)..

### **Lung**

Histological analysis of rat lung showed the usual mammalian organization into alveolar ducts, alveolar sacs and hundreds of interconnected thin walled capillaries filled with variably sized individual air-filled spaces. The alveoli were mostly composed of simple squamous alveolar epithelial cells with scattered cuboidal pneumocytes (Figure 15, 16).

The pulmonary parenchyma contained numerous bronchioles lined by simple columnar to cuboidal epithelium and surrounded by smooth muscle fibers (Figures 17, 18). The interalveolar connective tissue septa contained abundant blood capillaries, collagen fibers, and scattered leukocytes. Mild infiltration of inflammatory cells and macrophages was observed within the interstitial tissue in several sections (Figures 18, 19), In some regions, large blood vessels containing blood clots were observed adjacent to the alveolar structures (Figure 20).

### **Stomorphological Findings of the Respiratory System in Pigeons (*Columba livia*)**

#### **Upper and Lower Larynx**

The upper larynx of the pigeon was lined by pseudostratified ciliated columnar epithelium containing numerous goblet cells. The underlying lamina propria consisted of loose connective tissue rich in blood capillaries and scattered leukocytes. Numerous mucous glands were observed within the lamina propria and submucosal layers, frequently associated with lymphocytic infiltrations (Figures 21, 22, 23).

The wall of the upper larynx also contained abundant collagen fibers and bundles of skeletal muscle fibers embedded within connective tissue stroma (Figure 24). Hyaline cartilage surrounded by a distinct perichondrium was observed in the deeper layers of the laryngeal wall (Figures 21, 23).

The lower larynx (syrinx) exhibited extensive hyaline cartilaginous structures containing numerous chondrocytes embedded within a homogeneous cartilage matrix. These cartilages were surrounded by dense and loose collagenous connective tissue containing small blood vessels (Figures 25, 26, 27). The mucosal lining consisted primarily of pseudostratified ciliated columnar epithelium with varying degrees of leukocytic infiltration within both the epithelium and the underlying connective tissue (Figures 28, 29).

Additional sections demonstrated the presence of stratified squamous epithelium associated with well-developed skeletal muscle bundles, mucous glands, blood vessels, macrophages, and infiltrating leukocytes within the laryngeal wall (Figures 30, 31, 32, 33).

#### **Trachea**

The trachea of the pigeon was lined predominantly by pseudostratified ciliated columnar epithelium resting on a loose connective tissue lamina propria rich in blood vessels, mucous glands, collagen fibers, and infiltrating leukocytes (Figures 34, 35, 36, 37).

The submucosal layer contained complete hyaline cartilaginous rings surrounded by a well-developed perichondrium. Numerous chondrocytes with darkly stained nuclei occupied distinct lacunae within the cartilage matrix (Figures 38, 39, 40). The outer adventitial layer consisted of connective tissue containing adipose tissue, macrophages, blood vessels, and inflammatory cells (Figures 41, 42).

### **Lung**

Histological examination of the pigeon lung revealed a highly vascularized respiratory parenchyma displaying a spongy appearance. Numerous air spaces were lined by simple squamous and cuboidal epithelial cells and separated by thin interstitial septa containing blood capillaries and connective tissue elements (Figures 43, 44, 45).

Large air sacs and alveolar-like air spaces were observed in association with bronchiolar structures and numerous blood vessels. The interstitial tissue frequently contained leukocytes and macrophages distributed among the respiratory structures (Figures 46, 47, 48).

Wide air channels surrounded by multiple small air spaces were evident throughout the pulmonary tissue. These structures were associated with congested blood capillaries and extensive vascular networks, indicating the high respiratory capacity of the avian lung (Figures 49, 50, 51).

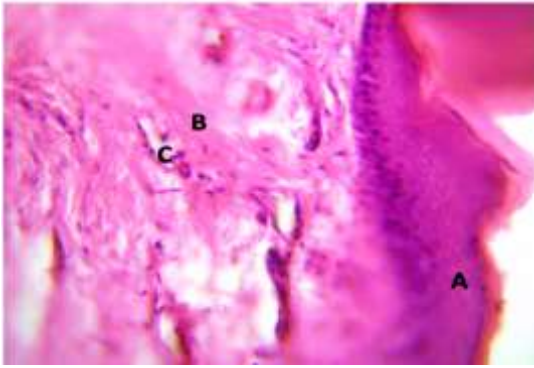


Fig. (1) It shows stratified keratinized squamous epithelium (A), The main surface contained colloid fibrous tissue (B) and white blood cell proliferation (C)/ (H & E x40).

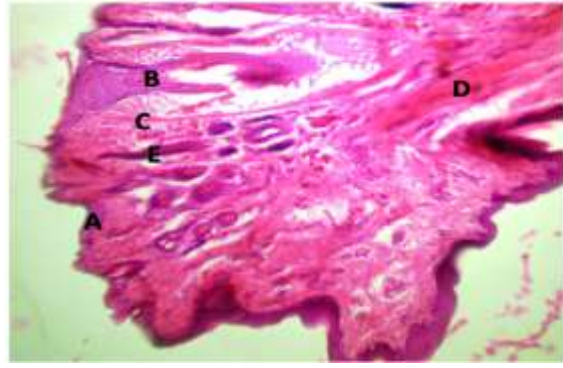


Fig. (2) Skin tissue in the nasal cavity of a rat containing stratified squamous epithelium (A), columnar epithelial papillae (B), bundles of colloidal fibers (C), bone tissue (D), hair follicles (E)/ (H & E x10).

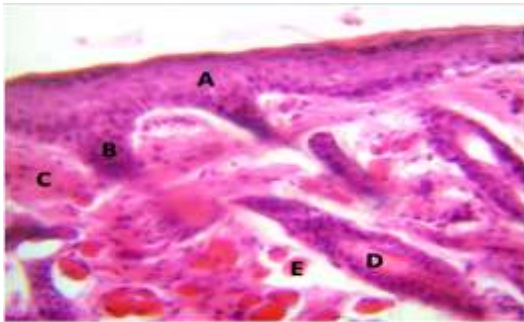


Fig. (3) The entrance to the nasal cavity in the rat, containing stratified squamous epithelium (A), epithelial papillae (B), bundles of colloidal fibers in the primary lamina (C), hair follicles (D), scattered skeletal muscle fibers (E)/ (H & E x40).



Fig. (4) The submucosa in the nasal cavity of the rat shows the compaction of mucous glands (A), bundles of colloidal fibers (B), and a cellular collection of egg blood between the glands (C)/ (H & E x40).

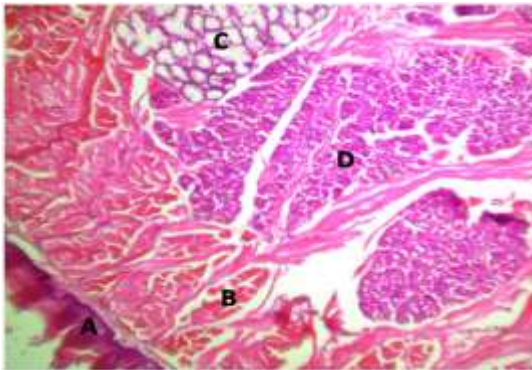


Fig. (5) Nasal cavity tissue showing stratified squamous epithelium (A), bundles of dense colloid fibers (B), mucous glands (C), serous glands (D)/ (H & E x10).

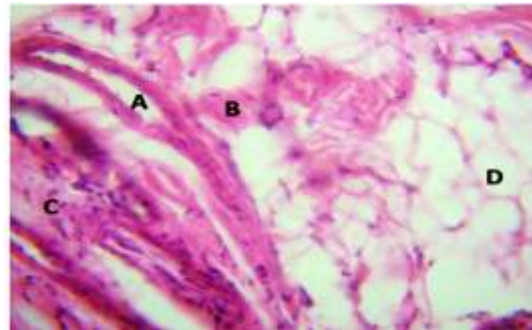


Fig. (6) The nasal cavity in the rat shows blood plexuses (A), blood vessels congested with blood (B), infiltration of white blood cells and phagocytes (C), adipose tissue (D)/ (H & E x40).

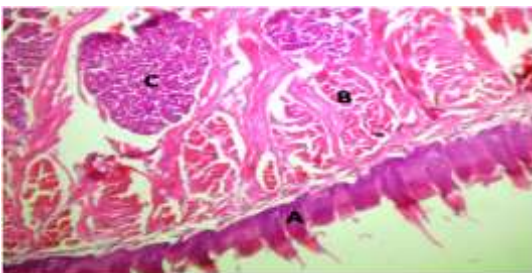


Fig. (7) The skin epithelium at the entrance of the nose contains stratified squamous epithelium with pointed papillae (A), bundles of dense colloid fibers (B), and mucous glands (C)/ (H & E x40).

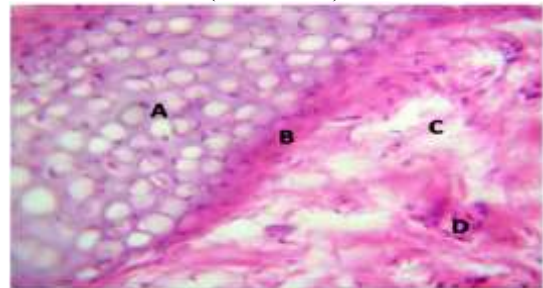


Fig. (8) It shows extensive hyaline cartilage with vacuole-shaped chondrocytes (A), chondrocyte periosteum (B), and bundles of collagen fibers (C)/ (H & E x40).

papillae (A), bundles of dense colloid fibers in the primary layer (B), lymphocytes in the form of a nodular cluster (C)/ (H & E x10).

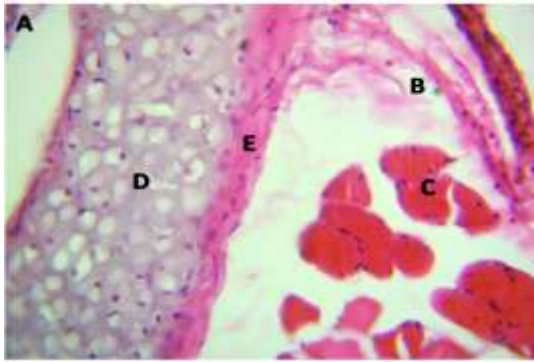


Fig. (9) Rat laryngeal tissue showing stratified squamous epithelium (A), loosened colloid fibers (B), loosened skeletal muscle fibers (C), hyaline cartilage ring (D), fibrocartilaginous periosteum (E)/ (H & E x40).

loosened colloidal fiber bundles (C), scattered white blood cells (D)/ (H & E x40).

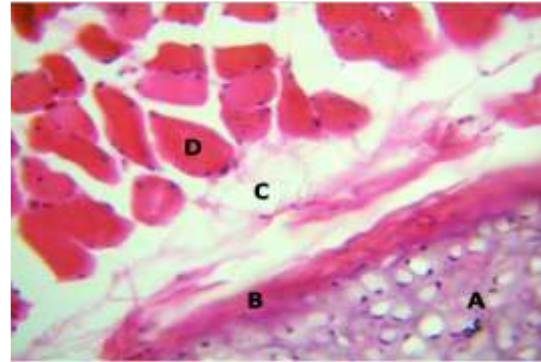


Fig. (10) The hyaline cartilaginous ring of the rat larynx shows (A) the dense colloid fiber bundles of the perichondrium (B) loose connective tissue in the submucosa (C) skeletal muscle fiber layer of the laryngeal wall (D)/ (H & E x40).

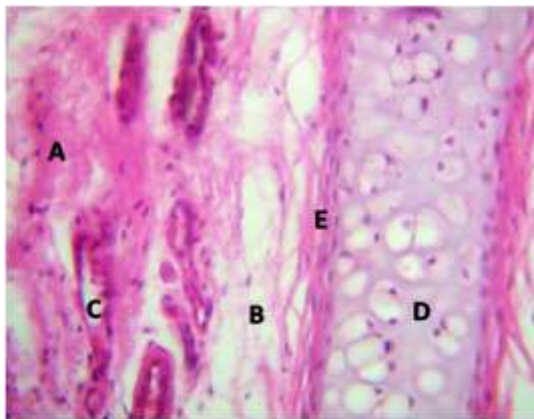


Fig. (11) The glial fiber bundles in the primary page of the rat trachea are shown (A) The primary page contains glial fiber bundles (B) Blood vessels surrounded by white blood cell infiltration (C) Hyaline cartilage ring (D) Chondromalacia (E)/ (H & E x40).

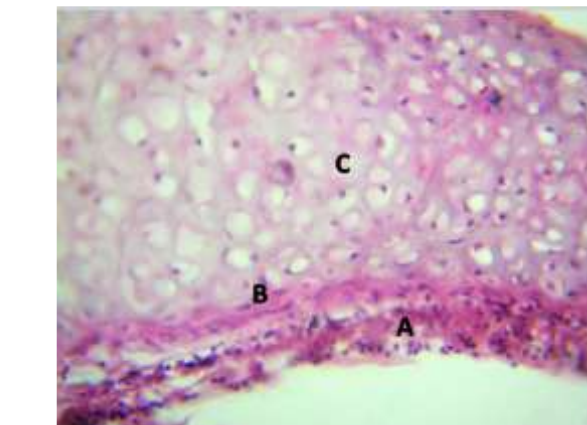


Fig. (12) Tracheal epithelium in the rat with pseudo-columnar squamous epithelium (A) White blood cell infiltration at the epithelium and around the chondrocyte periosteum (B) Wide hyaline cartilage with compaction of vacuole chondrocytes (C)/ (H & E x40).

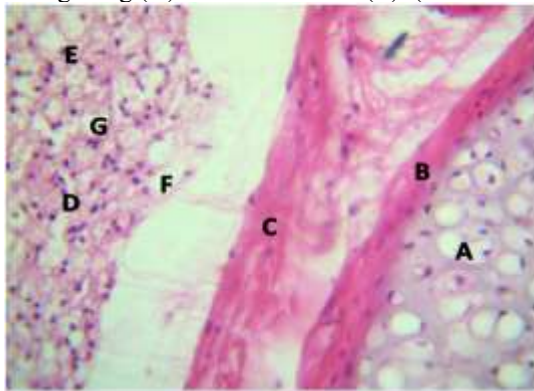


Fig. (13) The hyaline cartilage of the rat trachea shows (A) fibrochondral periosteum (B) bundles of colloid fibers with fibroblasts in the submucosa (C) the outer layer composed of loose connective tissue and leukocyte infiltration (D) macrophages (E) fat cells (F) bloodless capillaries (G)/ (H & E x40).

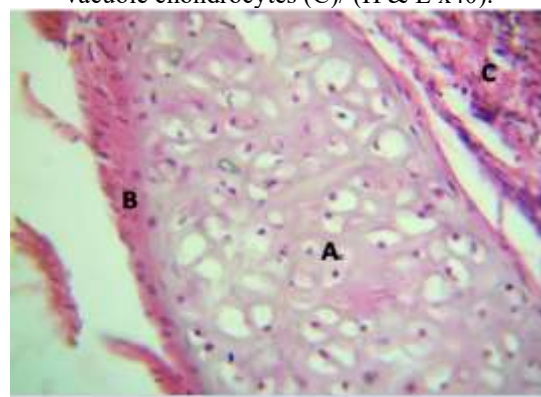


Fig. (14) Tracheal tissue in rats showing a wide cartilaginous ring with compaction of vacuole chondrocytes (A), perichondrium (B), bundles of muscle fibers (C)/ (H & E x40).

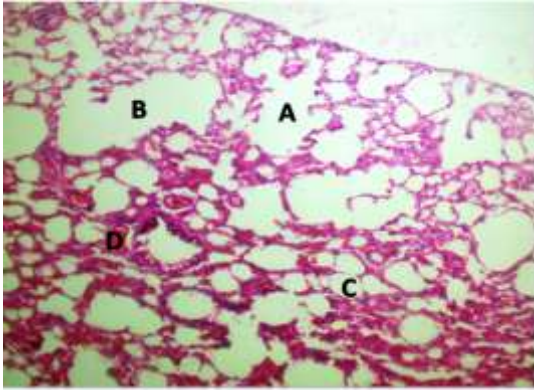


Fig. (15) Rat lung containing alveolar sacs (A), alveolar ducts (B), small air alveoli (C), blood capillaries with white blood cell infiltration in the interstitial tissue(D)/ (H&Ex40)

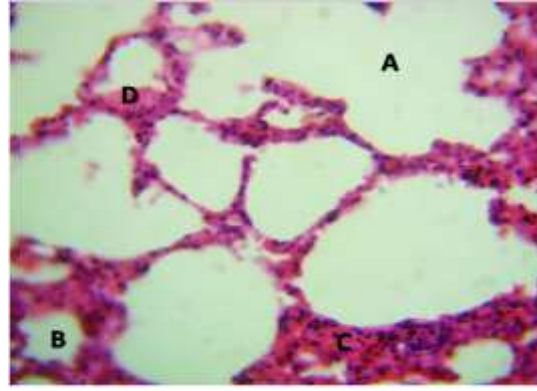


Fig. (16) Large air sacs lined with alveolar cells (A) Alveoli (B) Loose connective tissue containing white blood cells (C) Blood capillaries (D)/ (H & E x40).

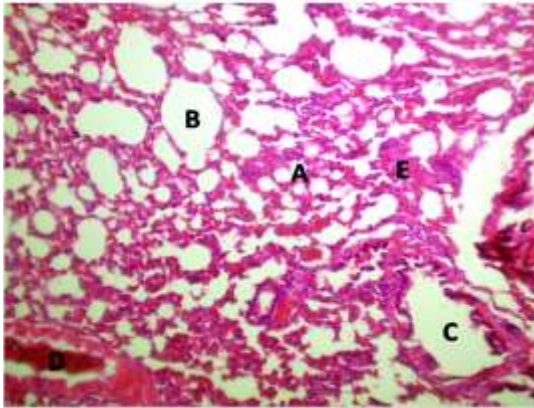


Fig. (17) A section of the lung in rats containing small air sacs (A), alveolar sacs (B), bronchioles (C), blood vessels congested with blood (D), interstitial tissue composed of thickened connective tissue fibers (E)/ (H & E x40).

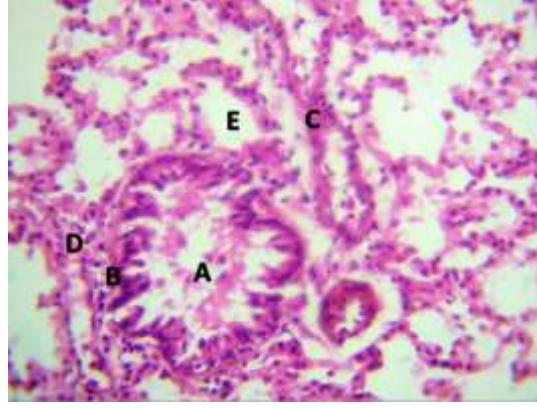


Fig. (18) Rat lung tissue shows the presence of bronchioles lined with simple columnar cells (A) and surrounded by smooth muscle fibers (B), thickening of the fibrous interstitial tissue (C), infiltration of white blood cells (D), and alveoli lined with squamous and simple columnar cells (E)/ (H & E x40).

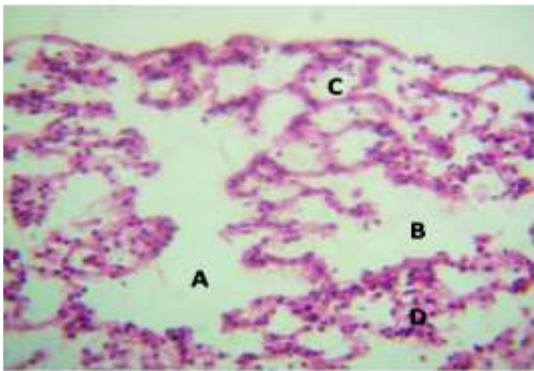


Fig. (19) Rat lung tissue with a large alveolar duct (A) connected to alveolar sacs (B), small air sacs (C), and loose connective tissue with white blood cell infiltration (D)/ (H & E x40).

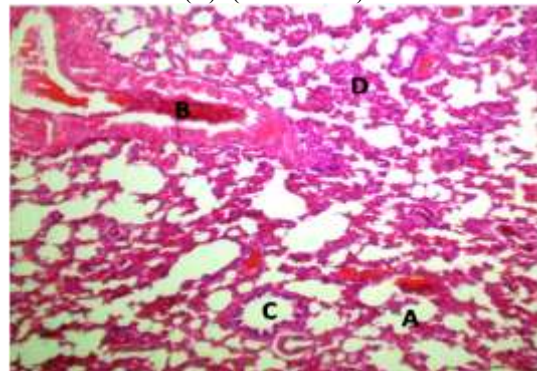


Fig. (20) Lung tissue showing the continuity of the alveoli with each other (A) Large blood vessel containing a blood clot (B) Bronchioles lined with simple cuboidal cells (C) Thickening of the interstitial tissue between the alveoli (D)/ (H & E x40).

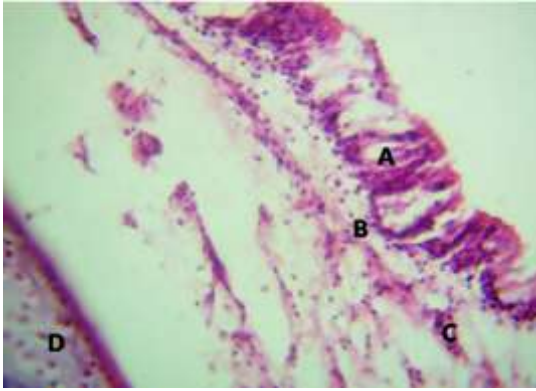


Fig. (21) The upper laryngeal epithelium of birds is shown with mucous casing cells between them. (A) The main surface contains an infiltration of white blood cells. (B) Blood capillaries. (C) Hyaline cartilage ring. (D)/ (H & E x40).

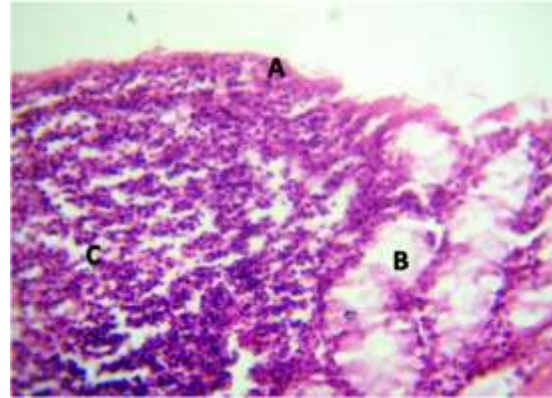


Fig. (22) The section shows pseudostratified columnar epithelium of the upper larynx of birds (A), mucosal glandular units (B), nodular lymphoid infiltration in the primary (C)/ (H & E x40).

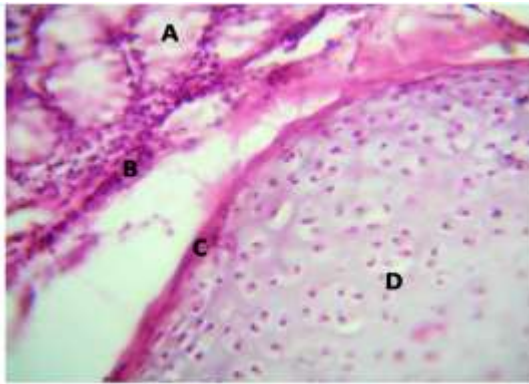


Fig. (23) Mucous gland compaction in the primary page of the upper larynx of birds (A) White blood cell infiltration under the glands (B) Hyaline cartilage in the submucosa (C) Chondroperioosteum (D)/ (H & E x40).

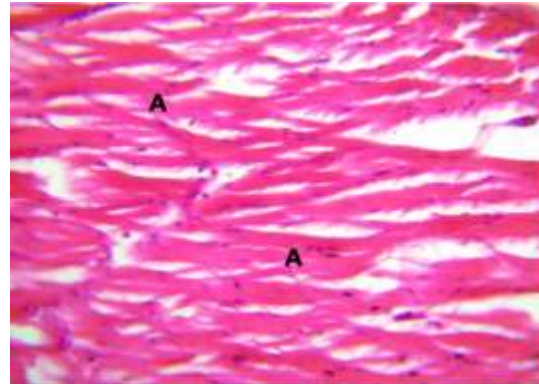


Fig. (24) Bundles of connective fibers with loosened skeletal muscle fibers in the upper larynx wall of birds (A)/ (H & E x40).

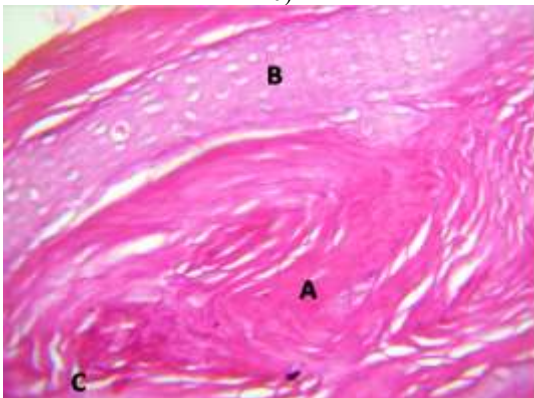


Fig. (25) The larynx shows bundles of dense colloid fibers (A) surrounded by hyaline cartilage in the form of a twisted band (B) in addition to the presence of small blood vessels (C)/ (H & E x40).



Fig. (26) The pigeon's larynx shows extensive hyaline cartilage (A), simple necrosis of the ground substance (B), perichondrium (C), loosened bundles of colloidal fibers (D), blood capillaries around the cartilage (E)/ (H & E x40).

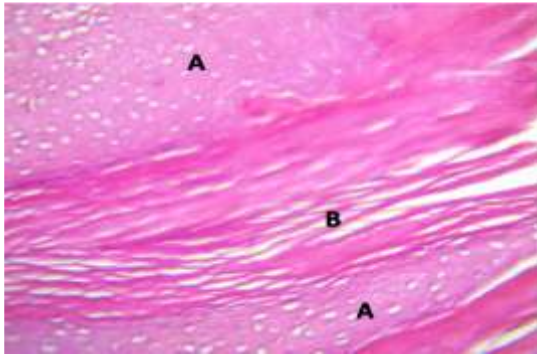


Fig. (27) The tissue shows two rows of hyaline cartilage of the lower larynx in the pigeon (A) surrounded by bundles of loosened colloid fibers (B)/ (H & E x40).

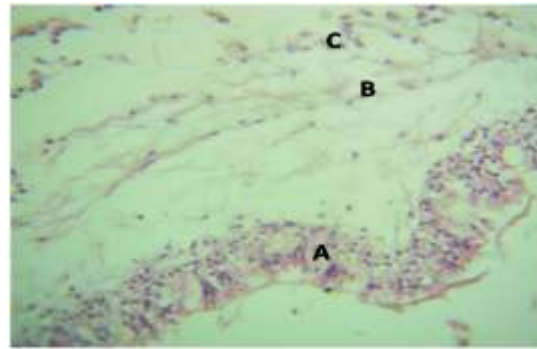


Fig. (28) (A) Pseudostratified columnar epithelium with white blood cells. (B) The main page with loose connective tissue. (C) Connective tissue cells and white blood cells. (H & E x40).

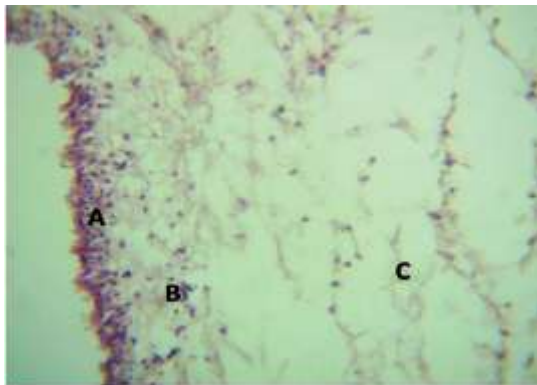


Fig. (29) Lower laryngeal epithelium of pigeons, pseudostratified columnar (A) Infiltration of white blood cells under the epithelium (B) Loose connective tissue in the baseline (C)/ (H & E x40).

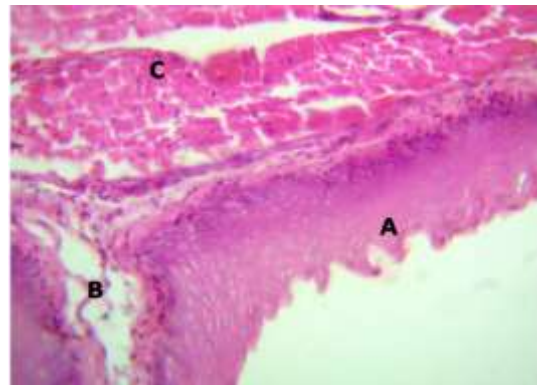


Fig. (30) It shows stratified squamous epithelium with short papillae on its surface (A) the main page and contains loose connective tissue (B) bundles of skeletal muscle fibers (C)/ (H & E x40).

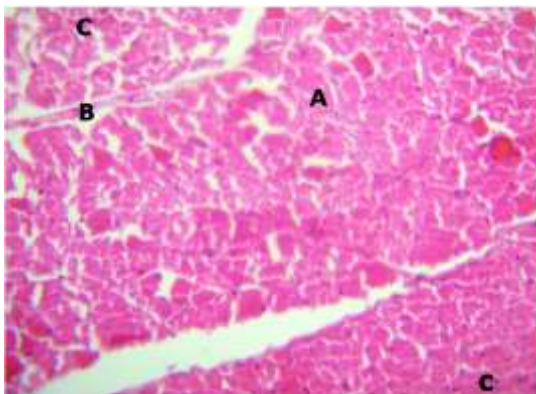


Fig. (31) Lower larynx wall containing (A) skeletal muscle fibers, (B) fascia, white blood cells and connective tissue cells (C)/ (H & E x40).

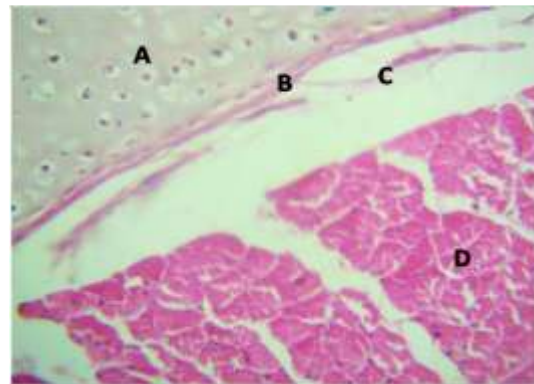


Fig. (32) Lower laryngeal wall containing a hyaline cartilage ring (A), cartilaginous periosteum (B), loose connective tissue in the submucosa (C), bundles of skeletal muscle fibers (D)/ (H & E x40).

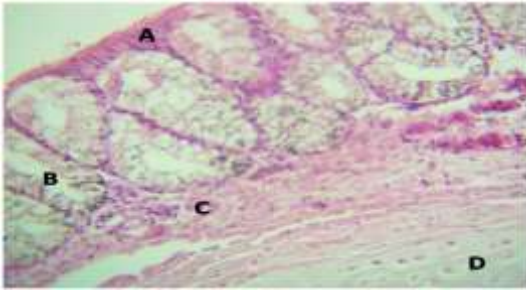


Fig. (33) Lower laryngeal tissue covered with keratinized squamous cells (A) tubular mucous glands in the primary (B) leukocyte infiltration (C) capillaries under the bases of the glands (D) hyaline cartilage (5)/ (H & E x40).

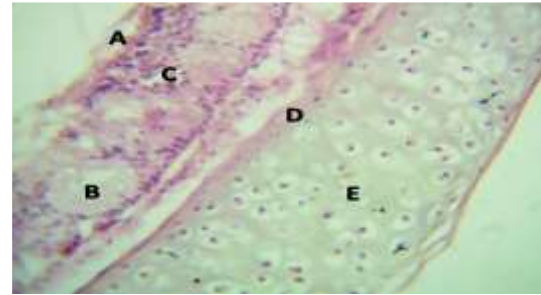


Fig. (34) The stratified columnar epithelium shows (A) mucous glands (B) the main page with infiltration of white blood cells (C) periosteum of the chondrocytes (E) hyaline cartilage (D)/ (H & E x40).

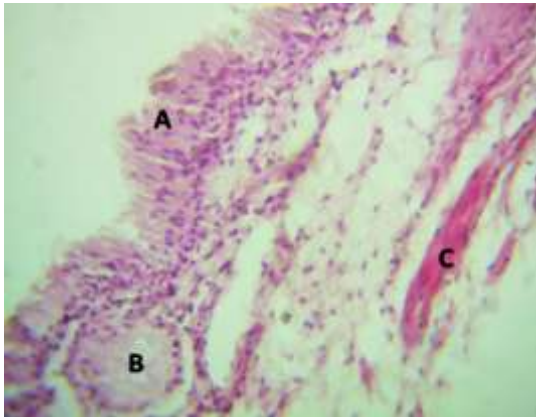


Fig. (35) Section showing the respiratory epithelium of pigeons (A) Mucous glands in the main page (B) Blood vessels and bundles of colloidal fibers (C)/ (H & E x40).

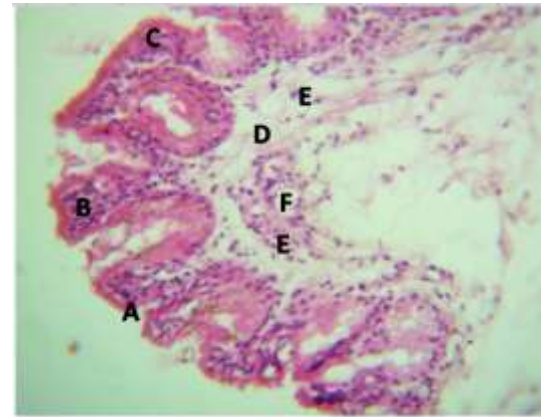


Fig. (36) The tracheal tissue of the pigeon shows mucoepithelial folds (A) pseudostratified columnar epithelium (B) keratinized squamous epithelium (C) the primary surface containing loose connective tissue (D) infiltration of leukocytes and phagocytes (E) bloodless capillaries (F)/ (H & E x40).

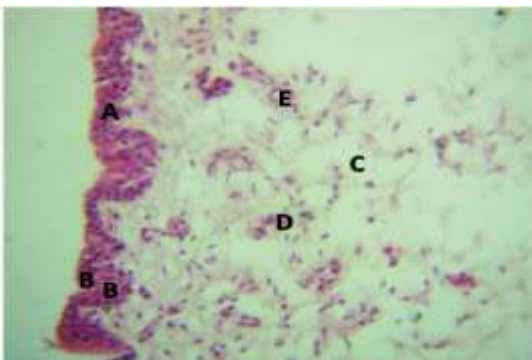


Fig. (37) It contains columnar epithelial tissue that is applied to the tracheal tissue in the pigeon (A) Epithelial folds and grooves (B) Loose connective tissue in the primary surface and it contains infiltration of white blood cells (C) Phagocytic cells (D) Microcapillaries (E)/ (H & E x40).

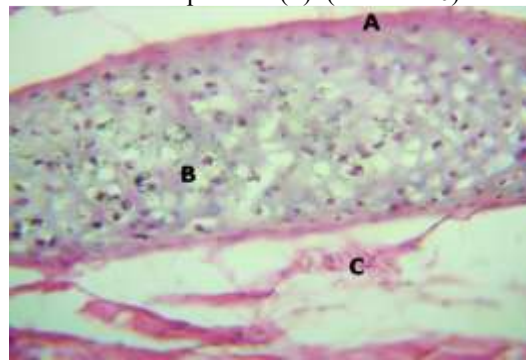


Fig. (38) The perichondral trachea shows (A) cartilage cells (B) and loose connective tissue (C)/ (H & E x40).

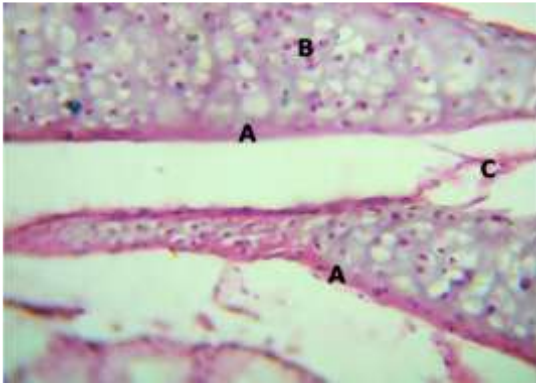


Fig. (39) The trachea shows two rows of hyaline cartilage surrounded by perichondrium (A) chondrocytes with dark-stained nuclei (B) interchondral tissue (C)/ (H & E x40).

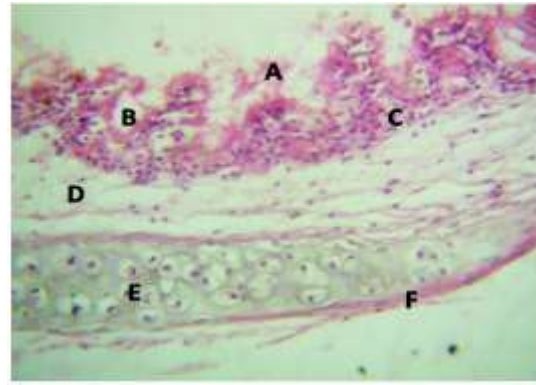


Fig. (40) The pigeon trachea shows a pseudostratified columnar epithelium in the form of folds (A), grooves between the folds (B), leukocyte infiltration at the base of the epithelium (C), loose connective tissue in the primary layer (D), hyaline cartilage ring in the submucosa (E), fibrocartilage periosteum around the ring (F)/ (H & E x40).

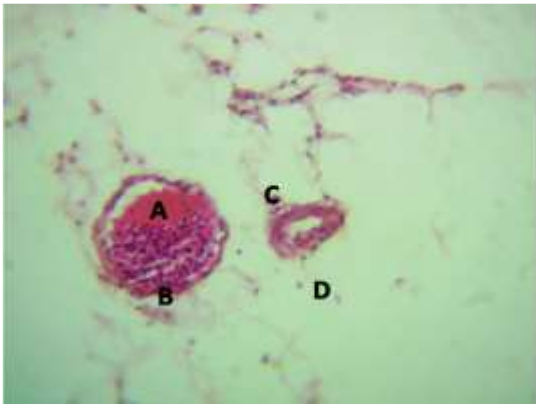


Fig. (41) The outer layer of the pigeon trachea shows blood vessels congested with blood (A) white blood cells (B) phagocytic cell (C) fatty tissue (D)/H&Ex40

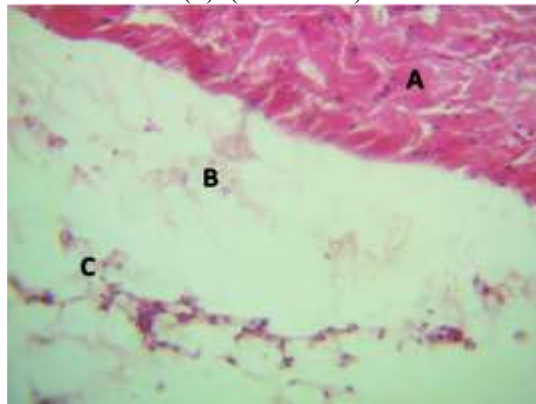


Fig. (42) (A) Bundles of colloidal fibers in the tracheal wall. (B) Loose connective tissue in the outer layer. (C) White blood cells and macrophages. (H & E x40).

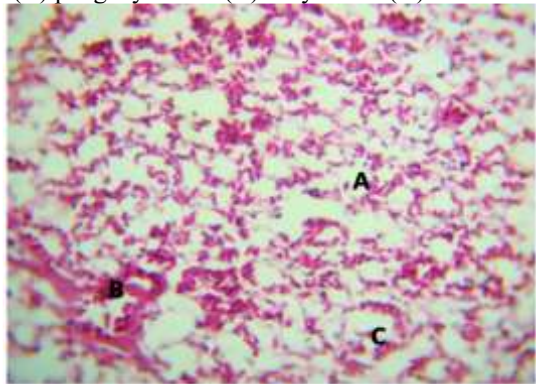


Fig. (43) The pigeon's lung, which contains multiple air alveoli (A), small blood vessels (B), and alveolar cells in the alveolar wall (C)/ (H & E x40).

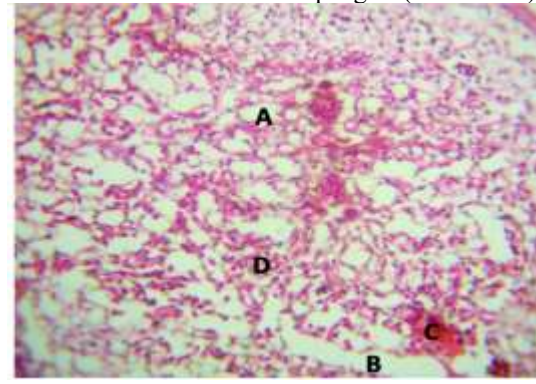


Fig. (44) The lung tissue in the pigeon shows the spongy pattern of the alveoli (A) alveolar duct (B) blood vessels congested with blood (C) white blood cell infiltration (D)/ (H & E x40).

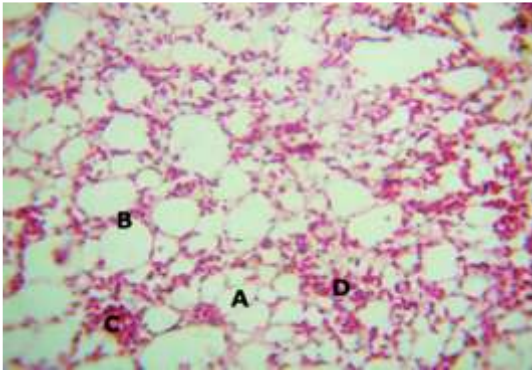


Fig. (45) The spongy pattern of the alveoli shows (A) cuboidal squamous alveolar cells (B) microcapillaries (C) leukocyte infiltration (D)/ (H & E x40).

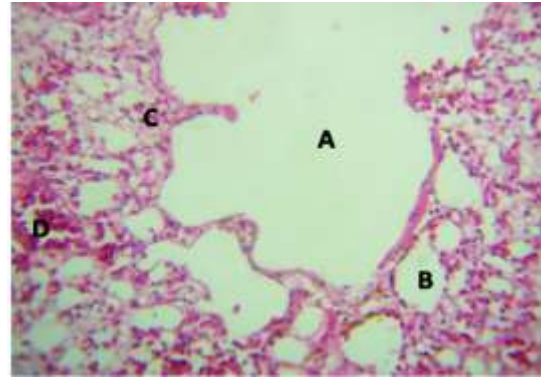


Fig. (46) Large alveolar sac in the pigeon lung (A) Alveoli lined with alveolar squamous and cuboidal cells (B) Infiltration of white blood cells and phagocytes (C) Bronchial airway (D)/ (H & E x40).

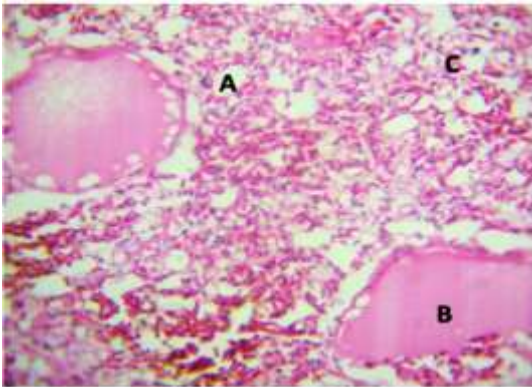


Fig. (47) Lung tissue in pigeons shows small air alveoli (A), large blood vessels filled with decomposed blood with air bubbles inside them (B), infiltration of white blood cells and phagocytes in the interstitial tissue (C)/ (H & E x40).

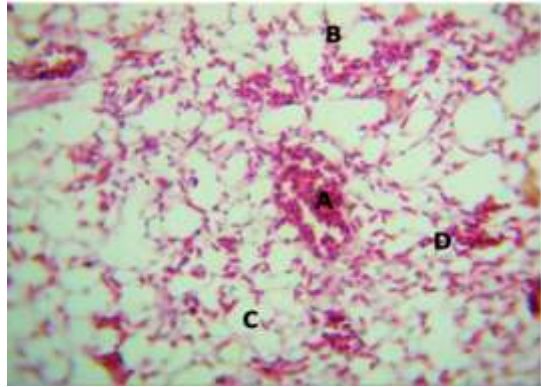


Fig. (48) Blood vessels congested with blood in the lung tissue of pigeons (A) bronchus (B) alveoli (C) infiltration of white blood cells and phagocytes in the interstitial tissue (D)/ (H & E x40).

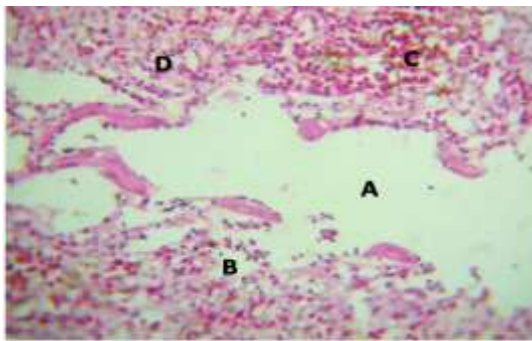


Fig. (49) Lung tissue in the pigeon with a wide alveolar duct (A) air alveoli (B) blood congestion in the capillaries (C) white blood cell infiltration in the interstitial tissue (D)/ (H & E x40).

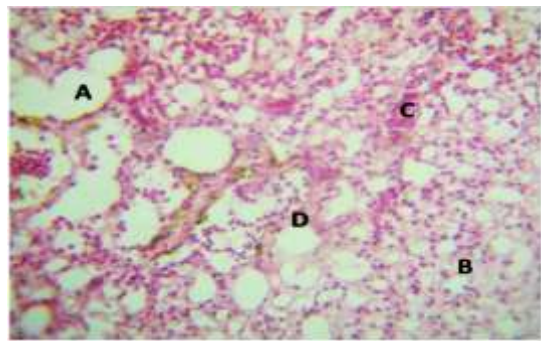


Fig. (50) Lung tissue in the pigeon with numerous alveolar sacs (A) small air alveoli of a spongy pattern (B) blood capillaries congested with blood (C) massive infiltration of white blood cells in the interstitial tissue (D)/ (H & E x40).

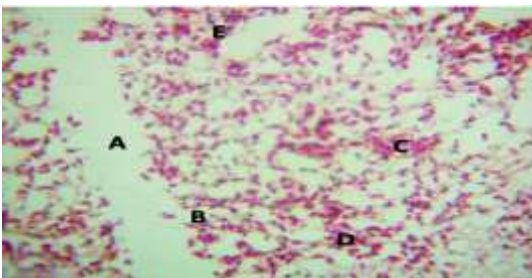


Fig. (51) Lung tissue in the pigeon containing an alveolar duct (A), air sacs connected to the alveolar duct (B) and interstitial tissue infiltration (C)/ (H & E x40).

(B), small blood capillaries congested with blood (C), white blood cells (D), phagocytic cells (E)/ (H & E x40).

## Discussion

The current study showed marked histomorphological variations in the respiratory system of male albino rat (*Rattus norvegicus*) and pigeons (*Columba livia*), resonates with unique air breathing mechanism utilized by mammal vs. bird species, respectively. In rats, the respiratory tract exhibited common mammalian configuration of tidal ventilation with a conducting portion covered by protective respiratory epithelium and pulmonary portion consisting of bronchioles along an alveolar duct-alveolar sac-aceptriable systemic significance. This was shown to correlate with a more widely defined mammaliandesign for respiration, whereby ventilation and gas exchange are reliant upon the cyclicalprocess of alveolar distension at inspiration via the upper airway (Phyu et al., 2023; Mulka et al., 2026).

The structure of nasal cavity in rats revealed that keratinized stratified squamous epithelium is present at the vestibular region and associated with hair follicles (GF) while dense collagen fibers persist along rich vascular plexuses perpendicular to an epithelial surface which shows it protects, but also conditions. Functional organization is vital considering that the anterior nasal region serves as a first line of defense to inhaled particles while these glandular and vascular components are responsible for holding mucus, humidifying air passages along with warming it up and filtration functions. Nonetheless, the presence of scattered leukocytes and lymphoid aggregations within lamina propria might represent subtle local mucosal immune surveillance; this can be identified focal.(Herbert *et al.*, 2017; Phyu *et al.*, 2023).

Rats exhibited grossly extensive hyaline cartilage with perichondrium, collagenous connective tissue and skeletal muscle bundles in the larynx. This arrangement of this structure correlates with the bivalent relationship between airway patency and phonation that is held in mammals, shared by their larynx. The presence of skeletal muscle fibers circumferentially around the laryngeal wall suggests that flexion/extension and rotational movement capability for airway lumen control are important in modulating respiratory function during swallowing or breathing events to protect lower airways from aspiration risk. Previous work describing leukocytes and macrophages in or around connective tissue may also represent normal resident immune cells, or mild local tissue response due to continuous exposure of respiratory mucosa to airborne antigens (Herbert *et al.*, 2017).

The luminal surface of the rat trachea was covered by a pseudostratified columnar respiratory epithelium supported by multiple large hyaline cartilage rings separated from surrounding fibrous perichondrium. Loosely arranged connective tissue interspersed with blood vessels, macrophages and infiltrating leukocytes were present in both the lamina propria and submucosa. These observations are compatible with mammalian conducting airways structure, which contains a mucociliary epithelium and other cell types underlying it to maintain patency & support functionally beneficial cilia-assisted clearance. Only one of the rare tissues in this region, hyaline cartilage (Herbert et al. 2017; Mulka et al.,2026).

Of particular interest here, pulmonary organization in histologically normal rats was quite highly structured within a lobular representation including not just bronchioles but also alveolar duct and sac as well with variable sized alveli lined mainly by simple squamous but containing some cuboidal pneumocytes. The reasoning for this histological pattern is thought to be that it closely resembles the mammalian way of gas exchange, with well developed alveoilthat provides a large surface area and short distance from air (gas) in between cells into blood. Many capillaries in the interalveolar septa not only perform their function to diffuse gases effectively but also support better diffusion of oxygen and carbon dioxide, defending against complexity as a consequence; thus confirming functional coupling between alveoli structure (Tsuda & Henry, 2023)

Collagen fibers, blood capillaries and scattered leukocytes macrophages were found in interstitial tissue from rat lungs by this study. Mild interstitial leukocytic infiltration and focal thickening of the interalveolar septa, on other hand may indicate local immune activity or slight tissue response following exposure under laboratory conditions or environmental circumstances respectively. With the exception of a foot print ( $\leq 2\text{mm}$ ) in an arachidonic chromatographic fold, extensive superficial epithelial destruction and inflammation induced edema or multiple inflammatory consolidation considered as mild histological alterations rather than diagnostic pathologic lesions. As such, these interpretations are confirmed with research studies showing that normal lung microarchitecture (such as alveolar septa and air blood barrier is required for maximum efficiency. :(Moserochi, 2023; Mulka et al., 2018)

The upper larynx epithelium appeared to be pseudostratified ciliated columnar type with goblet cells and followed by loose connective tissue which includes mucous glands & blood capillaries as well limited infiltration leukocytes. These traits suggest the bird upper respiratory tract serves as a high resistance airway for mucosal surface secretion and conditioning of inhaled air. The participation of mucous glands and ciliated epithelium is conducive to the effect of mucociliary clearance, and lymphoid infiltration in lamina propria may be a local immune defense against inhaled foreign particles and microorganisms. (Al-Taai 2021; Shakir 2022). Pigeon lower larynx or syrinx revealed that it consisted of various anatomical structure components: hyaline cartilage, dense collagenous connective tissue, bundles of skeletal muscle and mucous gland (Muneer & al., 2014) blood vessels; macrophages and leukocytes. You are basically trained for this organization because

syrinx is the primary vocal organ of birds, and it usually located near tracheobronchial junction. Cartilage provides structural support, while the components of skeletal muscle and connective tissue influence vibration/sound control. Thus, these findings corroborate results from anatomical studies detailing how specialized cartilaginous and membranous components of the pigeon syrinx form a tracheobronchial-type sound organ (Ibrahim *et al.*, 2020; Karaavci, 2024).

The trachea of the pigeon was entirely consisted of psudostratified ciliated columnar epithelium, mucous glands, loose connective and hyaline cartilage rings. Birds (horozlar), on the other hand, have tracheas founded in morphologies that differ from larval mammals and posterior to incomplete C-shaped cartilage rings. Unlike in mammals, pigeons have closed cartilaginous rings that increase rigidity and resistance to collapse allowing for pronounced unidirectional airflow between the lungs and air sacks in birds (Redfern *et al.* †2017). This design mimics the functional requirements of avian respiration and agrees with previous data that reported a completely cartilaginous prae-branchial segment from below one to pairs of primary bronchi traversing through several defined rings (Al-Taai, 2021; Karaavci, 2024).

The most superficial layer of the pigeon trachea was composed with connective tissue containing blood vessels, adipose tissue macrophages and leukocytes. These components imply that the tracheal wall is not merely a mechanical duct for conducting air, but could deserve to be characterized as metabolically active tissue with vascular and immune elements. The leukocytes and macrophages present in mucosae as well as adventitia could be involved in local defense mechanisms, especially because pigeons are at a high environmental exposure to airborne dust, fungal spores or other particles. Microbial colonization of the trachea and lungs is apparent in different kinds of birds, wherein those species cohabiting with pigeons have benefitted from this respiratory immune surveillance (de Melo-Neto *et al.*, 2022).

Pigeon lung had a spongy parenchymal appearance with many air spaces, thin interstitial septa, abundant blood capillaries and bronchiolar structures intermixed among the connective tissue as well leucocytes (pigeons possess heterophils) and macrophages scattered throughout the section. These spaces, which initially appear less defined under light microscopy and more alveolar-type structure than that of the mammalian lung. Birds have fully rigid parabronchial lungs, in which gas exchange occurs through air capillaries and blood capillaries but not true mammalian alveoli. Hence, we conclude that the spongy pattern observed in these sections of pigeon lung should not be interpreted as a true alveolar system identical to mammals but rather reflect some aspect of the avian parabronchial and capillary architecture (Maina, 2025; Schachner & Moore, 2025).

Indeed, one of the highest vascularities can be observed in pigeon lung tissue to ensure that air spaces are closely associated with blood capillaries for optimal gas exchange. This configuration is compatible with the respiratory system of birds, wherein lungs serve primarily as gas exchanges and air sacs function mainly to ventilate. This rigid lung and unidirectional airflow allow birds to keep a continuous flow of air through their gas-exchange regions, yielding highly efficient oxygen extraction compared with the tidal ventilation of mammals (Maina, 2025; Klein *et al.*, 2025).

By contrast, the rat lung is considered a mammalian bronchioalveolar model in which ventilation requires expansion and recoil of alveoli (a ballooning process), while with pigeon lungs gas exchange occurs associated with expansions of airways against rigid tissues instead. This basic difference accounts for the histological disparity between rats as observed in the present study, alveolar sacs and varied sizes of alveoli versus pigeons having a denser vascular, spongy respiratory tissue connected to airways canals/capillary networks. These differences highlight two independent evolutionary pathways for respiratory efficiency in endothermic vertebrates (Tsuda & Henry, 2023; Maina, 2025).

More substantial cartilaginous support in pigeon trachea and syrinx relative to rat trachea and larynx reflects the mechanical needs of avian respiration versus vocalization. Complete tracheal rings and syringeal cartilages in pigeons serve as mechanical support for sound production; however, rat tracheas have a more flexible airway structure supported by the incomplete cartilage to facilitate mammalian tidal breathing. Therefore, the histological structure of cartilage and connective tissue in both species is well related to their respiratory mechanics (Al-Taai, 2021; Karaavci, 2024).

The presence of leukocytes and macrophages in rat and pigeon respiratory tissues may be justified by the fact that environmental particles (especially carbon) or other antigens are constantly inhaled into their respiratory tract. Their widespread presence was observed more obviously in select sections of the trachea, larynx, and lung from pigeons that could be attributed to environmental exposure due to avian respiratory surfaces being open directly to airborne materials. This observation underpin that the respiratory mucosa not only roles in air conduction and gas exchange but also an important local immune defence house site (de Melo-Neto *et al.*, 2022; Mulka *et al.*, 2026).

Conclusion However, as for the present results indicate that male albino rat and pigeons reveal with characteristic morphological features in their respiratory system which include epithelial lining, cartilage organization including glandular distribution details {(hyperplastic)}and also some detail about pulmonary architecture (it maybe hyperplasia) if we can't detect any pathological change but it normal condition because measurement of precision is less representative than clinical status. The resulting differences in morphology and movement are intimately tied to the different functional demands of mammalian tidal ventilation relative to avian unidirectional airflow. Consequently, the histomorphologic characteristics of both species in this study

correspond to adaptive specializations in respiratory system and therefore provide unique information for comparative anatomy.

## Conclusion

The current comparative histomorphological examination revealed prominent structural variants in the respiratory system between male albino rat (*Rattus norvegicus*) and pigeons (*Columba livia*), which mirrors their functional and adaptational demands for mammalian & avian respiration.

The system adds up to the characteristic mammalian pattern, with a keratinized and glandular nasal mucosa in rats, larynx and trachea supported by hyaline cartilage including pulmonary parenchyma (bronchioles; alveolar ducts; alveolar sacs), multiple partitions lengthwise run between structures which are richly vascularised along its thin air-blood barrier tending towards tidal ventilation with large numbers of adaptations set at narrow physiological pressure differentials eliciting gas exchange efficiency from lung elasticity through cyclic expansion contraction.

On the contrary, pigeons featured many derived avian adaptations in their respiratory system, characterized by a simple pseudostratified ciliated respiratory epithelium with abundant mucous glands; complete cartilaginous tracheal rings oriented horizontally; specialized syrinx and richly vascularized pulmonary tissue with heterogeneous compact spongy organization features consistent with an adaptive pattern in birds for rigid lungs working at maximal efficiency to promote continuous unidirectional airflow aimed mainly on oxygen extraction.

Compared with human lungs, key observations included improved epithelio-mesenchymal organization, a more abundant distribution of cartilage and submucosal glands in asymmetric branching morphogenetic patterns as well as better connective tissue matrix structure or vascularization (in primate relative to mouse), alveolar type development versus microarchitecture demonstrated fundamental species differences between lung development models. All these histological variability appears to be structural adaptations of each species to their physiological needs and requirements.

In summary, these results provide further support that mammalian and avian respiratory systems have evolved separate morphological solutions for effective gas transfer; The data generated should highlight the comparative histology and adaptive functional morphology of vertebrate respiration: thus providing a foundation which may be valuable groundwork in veterinary anatomy as well as general evolutionary biology.

## Recommendations and Future Perspectives

1. More comparative histomorphological studies on more avian and mammalian species will better elucidate the evolutionary diversity of vertebrate respiratory adaptations.
2. Investigations employing histochemical, immunohistochemical and ultrastructural techniques are needed to better characterize these cellular/molecular differences within the tissues themselves.
3. The qualitative findings from the present study should be supported by quantitative morphometric analyses, such as measurements of epithelial thickness, cartilage dimensions and density analysis on glandular or vascular distribution/pulmonary structures.
4. We propose that comparative studies combining histological observation of tissues with the underlying physiological basis for function will be useful in elucidating one approximate correspondence between structural and functional patterns across vertebrate groups, although further work is required to resolve this issue.
5. How the avian syrinx and parabronchial lung structure serves in vocalizing, venting efficaciously during flight, as well as uniquely adapting to uptake and circulation oxygen through continued use is a compelling avenue of research that could be inspiring.
6. Future studies could therefore assess the effects of age, sex and environmental factors with respect to respiratory tissue configurations in mammals versus birds.

## Acknowledgments

The author gratefully acknowledges the assistance provided by the laboratory staff during the preparation and processing of histological specimens.

## Funding

This study was entirely self-funded by the researchers and received no external financial support.

## References

1. AL-Taai, S. A. (2021). Microscopic and morphometric study in trachea and lungs of adult Iraqi pigeon (*Columba livia*). *Syst Rev Pharm*, 12(2), 342-346.
2. de Melo-Neto, M. F., de Albuquerque Maranhão, F. C., da Silva Guimarães, P., & Silva, D. M. W. (2022). Mycobiota recovered from the trachea and lungs of pigeons (*Columba livia*) captured in a grain mill. *Research, Society and Development*, 11(3), e57211326802-e57211326802.

3. Dominelli, P. B., & Sheel, A. W. (2024). The pulmonary physiology of exercise. *Advances in physiology education*, 48(2), 238-251.
4. Herbert, R. A., Janardhan, K. S., Pandiri, A. R., Cesta, M. F., & Miller, R. A. (2018). Nose, larynx, and trachea. In *Boorman's Pathology of the Rat* (pp. 391-435). Academic Press.
5. Ibrahim, I. A. A., Hussein, M. M., Hamdy, A., & Abdel-Maksoud, F. M. (2020). Comparative morphological features of syrinx in male domestic fowl *Gallus gallus domesticus* and male domestic pigeon *Columba livia domestica*: A histochemical, ultrastructural, scanning electron microscopic and morphometrical study. *Microscopy and Microanalysis*, 26(2), 326-347.
6. Karaavcı, F. A., Koçyiğit, A., & Kanik, B. (2024). Morphological comparison of larynx, syrinx and trachea of some wild birds. *Harran University Journal of the Faculty of Veterinary Medicine*, 13(1), 48-55.
7. Klein, W., Pereira Ribeiro, V., & Bueno de Souza, R. B. (2025). Avian air sacs and neopulmo: their evolution, form and function. *Philosophical Transactions of the Royal Society B: Biological Sciences*, 380(1920).
8. Maina, J. N. (2022). Perspectives on the structure and function of the avian respiratory system: functional efficiency built on structural complexity. *Frontiers in Animal Science*, 3, 851574.
9. Maina, J. N. (2025). Structure and function of the avian respiratory system. *Philosophical Transactions of the Royal Society B: Biological Sciences*, 380(1920).
10. Meduri, G. U., & Torres, A. (2026). Evolutionary Integration and Glucocorticoid Regulation of the Respiratory System: Structure, Function, and Homeostatic Adaptation. *Medical Sciences*, 14(1), 90.
11. Miserocchi, G. (2023). The impact of heterogeneity of the air-blood barrier on control of lung extravascular water and alveolar gas exchange. *Frontiers in Network Physiology*, 3, 1142245.
12. Moussavi, Z. (2022). Anatomy and Physiology of Respiratory System. In *Fundamentals of Respiratory System and Sounds Analysis* (pp. 1-8). Cham: Springer International Publishing.
13. Mulka, K. R., Gruenwald, R. C., Yang, T. S., & Caswell, J. L. (2026). Microscopic anatomy of the lungs of domestic animals, mice, and rats. *Journal of Veterinary Diagnostic Investigation*, 10406387251413159.
14. Phyu, S. L., Turnbull, C., & Talbot, N. (2023). Basic respiratory physiology. *Medicine*, 51(10), 679-683.
15. Rekabdar, T., Yousefi, M., Masoudifard, M., Zehtabvar, O., & Ahmadpanahi, S. J. (2024). Computed Tomographic Anatomy and Topography of the Lower Respiratory System of the Mature Rat (*Rattus norvegicus*). *Archives of Razi Institute*, 79(5), 981.
16. Ritchison, G. (2023). Respiration. In *In a Class of Their Own* (pp. 1007–1084). Springer Nature Switzerland. <https://doi.org/10.1007/978-3-031-14852-17>.
17. Schachner, E. R., & Moore, A. J. (2025). Unidirectional airflow, air sacs or the horizontal septum: what does it take to make a bird lung?. *Philosophical Transactions of the Royal Society B: Biological Sciences*, 380(1920).
18. Shakir, E. (2022). Review on the morphological structures and histological features of the respiratory system in birds. *Acta Scientific Veterinary Sciences*, 4(10), 113–116.
19. Tsuda, A., & Henry, F. S. (2023). The effect of heterogeneity of the network of alveolar wall tissue on airflow, interstitial flow and lung biology. *Frontiers in Network Physiology*, 3, 1272172.